

Hydrodynamic Droplet Breakup Modeling in Liquid-Fueled Detonations

Stephan Agee
Texas A&M University
College Station, TX, USA

Manoj Paudel
Texas A&M University
College Station, TX, USA

Praveen Ramaprabhu
University of North Carolina Charlotte
Charlotte, NC, USA

Jacob McFarland
Texas A&M University
College Station, TX, USA

1 Introduction

Liquid-fueled detonations are a complex multi-scale multi-physics problem in which micron-sized liquid droplets must breakup, evaporate, and react at microsecond time scales. The development of detonation propulsion devices utilizing high-density liquid fuels requires an increased understanding of the droplet deformation and breakup processes. Contrary to gaseous detonations, liquid-fueled detonations are inherently heterogeneous and droplets must be heated, evaporated, and mixed with oxidizer before the fuel mass can react and sustain the detonation. Droplet vaporization is enhanced significantly by droplet breakup as the droplet is accelerated by the post-shock flow. These processes are innately coupled and occur at overlapping timescales.

The simple one-dimensional model provided by Zeldovich, Neumann, and Doring describes the detonation process as a steady shock wave moving at the Chapman-Jouget (CJ), followed by a finite reaction zone that is terminated at the CJ point. In order to sustain the detonation, fuel mass contained in droplets must evaporate and react before the CJ point. The leading shock wave is strong, traveling greater than Mach 6 for many hydrocarbon fuels, subjecting the fuel droplets to high velocity, order of 2000m/s , high temperature, order of 2000K , gas conditions [1]. Under these conditions the droplet interface will be unstable and subject to high heat transfer and evaporation rates. In addition to the leading shock, real-world detonations (2D and 3D) evolve a system on transverse shock waves which re-accelerate

the droplets in varying directions, creating complex and unsteady conditions under which the droplet evolves.

The stability of a droplet subjected to high velocity gas flow can be described by the Weber number, $We = \frac{\rho_g u_g^2 d_p}{\sigma}$, where ρ_g is the post shock gas density, u_g the relative velocity between the gas and droplet, d_p the droplet diameter, and σ the surface tension of the liquid. The breakup process has been grouped into several regimes by various authors [2]. For liquid-fueled detonation devices, droplet sizes of interest range from approximately $1 - 100 \mu m$. For these sizes We typically are on the order of $1E3-1E5$, putting them in what has been described by some as the catastrophic breakup regime.

Breakup models for the high We regimes are limited. Previous empirical models have been limited to lower We and have not been developed for the unsteady conditions found in detonations. One option to model breakup at high We is to use a theoretical model, which can be extended to a wide range of conditions. One such model is the Kelvin-Helmholtz (KH) Rayleigh-Taylor (RT) model, as described by Beale and Reitz [3]. In this model small child droplets are continuously stripped from the droplet surface by the KH instability (driven by shear forces) while simultaneously an RT instability evolves on the windward side of the droplet surface due to the pressure gradient (droplet acceleration), leading to a sudden breakup of the droplet core at a later time. This model has been applied in previous work [1, 4], but requires further development or calibration for new conditions.

This paper will examine the ability of a calibrated KHRT breakup model to reproduce detonation properties observed by comparing simulation and experimental results. The following sections will describe the experimental facility and results, discuss the calibration of the KHRT model, then present the results of simulation using the new model, and finally close with concluding remarks.

2 Experimental Results

Experimental results were obtained in a vertical 3.25m multiphase detonation tube (fig. 1). The detonation tube is comprised of an initiation, development section, test section, and finally an expansion tank. A custom designed particle seeder, housing nine piezoelectric oscillating mesh (POM) atomizers, sat atop the initiation section to produce a spatially uniform distribution of fuel particles. Within the particle seeder an assortment of 32 1/16" holes were arranged in annulus, simultaneously providing an inlet for O₂ gas and mitigating wall-particle collisions. A spark plug within the initiation section was used to ignite the combustible mixture. Following the initiation section, the initial wave propagates into the acceleration section where it encounters a Schelkien coil, assisting with the deflagration to detonation (DDT) process. The ensuing 1.5m long development section provides sufficient length for the incipient detonation wave to decay to a quasi-steady state. Lastly, the detonation propagates through the test sections and into the expansion tank filled with inert gas, extinguishing the wave. At the test section, Mie scattering and CH* chemiluminescence optical diagnostics were simultaneously executed to procure measurements of droplet breakup distances. A LaVision CX2-25MP camera was filtered with a $532 \pm 1nm$ bandpass filter, isolating the scattered light emission from a Litron Nano-T 532nm Nd:YAG laser. In addition, a high-speed Phantom T-3610 camera was filtered with a $430 \pm 5nm$ bandpass filter, segregating the light emissions for CH* radicals. The optically dense aerosol obscures the visualization of the leading shock wave, necessitating the use of CH* to sense the presence of chemical reactions. Coupling the two diagnostics permits a strong estimation of the total breakup distance. Droplet sizes were characterized in-situ within the detonation tube test section, using a TSI instruments Phase Doppler Particle Anemometer with an accuracy of $\pm 1.5 \mu m$. For the case presented here the droplet size distribution was found to have D10 and D32 diameters of $8.2 \mu m$ and $13.5 \mu m$ respectively. The equivalence ratio was measured by filling the tube to the initial conditions then evacuating the gas/droplet mixture

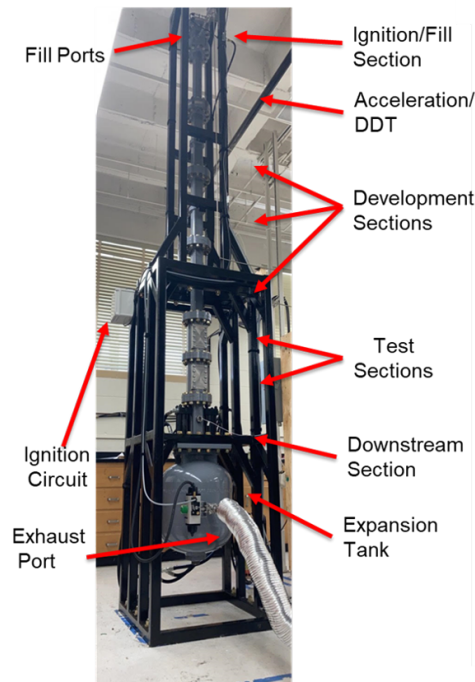


Figure 1: The Texas A&M Multiphase Detonation Tube.

through a filtration system. The filter droplet mass was weighed and the equivalence ratio measured to be 0.23 ± 0.05 .

Figure 2 shows a Mie-scattering image of the droplet field during droplet breakup. The location of the shock wave was found using CH^* images (marked by the sudden increase in CH^* intensity) and is shown as a dashed red line. It can be seen that the Mie-scattering signal does not initially increase after the shock wave, then it suddenly increases at a distance of $\approx 1.3\text{mm}$ behind the shock. This bright region persists for $\approx 2.5\text{mm}$ before scattered light emission are extinguished. One explanation for this behavior is that the KH instability, which is predicted to occur soon after shock passage, creates droplets that are too small to create significant scattered light as explained in previous work [5]. The rapid increase in brightness can be attributed to an RT breakup event, which creates larger child droplets that efficiently scatter light and greatly increase the total surface area for scattering. As the droplets breakdown into to smaller child droplets, they rapidly equilibrate with the gas velocity, causing them to increase in number density. This is analogous to the increase in gas density which occurs behind the shock front.

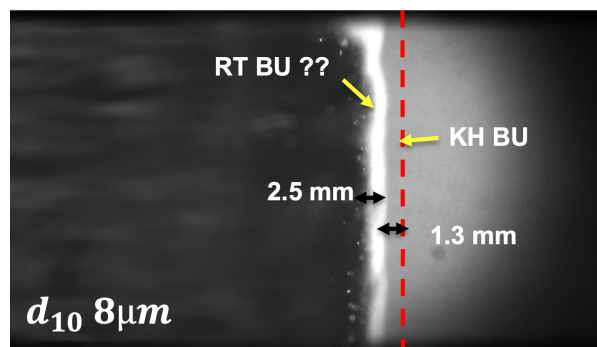


Figure 2: Mie Scattering images of droplets with $8\ \mu\text{m}$ piezoelectric atomizer

3 Simulations

3.1 Methods

The liquid fuel detonation simulation is carried out in a hydrodynamic code FLASH [6] using Euler-Lagrange method where the gas phase is solved in the Eulerian mesh and the droplets are evolved in Lagrangian fashion. The reactive Euler equations (1-4) with multiphase source terms are solved for the evolution of the gas phase and two way coupling between the gas and droplets is achieved through bilinear mapping of the multiphase source terms. The conservation equations without source terms is solved using directionally split Piecewise Parabolic Method (PPM) [7] and operator splitting is used to couple source terms. The details of overall solution procedure is presented in [4].

$$\frac{\partial \epsilon \rho_g}{\partial t} + \nabla \cdot \epsilon \rho_g \mathbf{v}_g = -M_p \quad (1)$$

$$\frac{\partial \epsilon \rho_g \mathbf{v}_g}{\partial t} + \nabla \cdot \epsilon \rho_g \mathbf{v}_g \mathbf{v}_g + \nabla P = -\mathbf{F}_p \quad (2)$$

$$\frac{\partial \epsilon \rho_g E}{\partial t} + \nabla \cdot (\epsilon \rho_g E + P) \mathbf{v}_g + P \frac{\partial \epsilon}{\partial t} = E_p \quad (3)$$

$$\frac{\partial \epsilon \rho_g Y_i}{\partial t} + \nabla \cdot \epsilon \rho_g Y_i \mathbf{v}_g = -M_{p,i} + \dot{\omega}_{rxn,i}, \quad \sum_{i=1}^n Y_i = 1 \quad (4)$$

For the reaction, a two-step reaction mechanism with two fictitious products and reaction rate of Arrhenius form given by $A \exp(-E_a/(RT))$ is developed to reproduce the ZND parameters obtained using the JetSurf2.0 reaction mechanism [8]. Table 1 presents the reactions and rate constants used. The molecular weight and enthalpy (NASA7 coefficients) of the products P₁ and P₂ are taken as the molar combination of representative equilibrium species as obtained by using JetSurf2.0 in Cantera [9], see Eqn 6.

Table 1: Reaction mechanism and Arrhenius rate constants

Reaction	Equation	A	b	Ea	Orders
R1	$\text{C}_{12}\text{H}_{26} + 18.5 \text{O}_2 \longrightarrow 38 \text{P}_1$	7.5E12	0	45,000	$[\text{C}_{10}\text{H}_{22}]^{0.25}, [\text{O}_2]^{1.5}$
R2	$1.3945 \text{P}_1 \rightleftharpoons \text{P}_2$	1E10	0	12,000	-

$$\text{P}_1 = 12 \text{CO} + 25 \text{OH} + \text{H} \quad (5)$$

$$\text{P}_2 = 10 \text{CO}_2 + 10.5 \text{H}_2\text{O} + 2 \text{CO} + 2.25 \text{O}_2 + 2.5 \text{H}_2 \quad (6)$$

3.2 Droplet Models

The droplets are evolved in time considering the deformation, drag, breakup and evaporation. Deformation of the droplet is calculated using the Taylor Analogy Breakup [10] model, using the non-dimensionalized form presented in Stefanitsis et al [11], which gives the instantaneous deformation ($Y = d_y/d_0$).

$$\ddot{y} + 4C_\delta \frac{\text{Oh}}{\sqrt{\text{We}}} \dot{y} + \frac{8C_k}{\text{We}} (y - 1) = 4C_f \quad (7)$$

where \dot{y} represents the derivative of y with respect to non-dimensional time $t^* = t/t_c$ where, t_c is the Ranger and Nichols time. The coefficient values of $C_\delta = 5$, $C_k = 8$ and $C_f = 1$ is used. The Y term is incorporated to get a dynamic drag model with drag coefficient given by Eqn 8 where $C_{d,sph}$ is the drag coefficient of sphere calculated using Kliachko's model.

$$C_d = C_{d,sph} \left[1 + 2.632 \left(1 - \frac{1}{y^6} \right) \right] \quad (8)$$

Evaporation of the liquid droplet is evaluated using Abramzon and Sirignano's model [12] and droplet atomization follows a modified version of the KHRT breakup model originally proposed by Reitz [13] and Beale and Reitz [3]. The coefficients of the modified KHRT model and its implementation are presented in Paudel and McFarland [4].

3.3 Results

The simulation is run in a 2D rectangular domain of size $262.2 \text{ cm} \times 5.7 \text{ cm}$ with reflecting walls, to mimic the detonation tube. Figure 3 shows the initial domain where the detonation is initiated by a sinusoidal-shaped region of high pressure and temperature premixed gas. The detonation begins in a premixed gaseous fuel and oxidizer region before transitioning to the particle containing region with no pre-vaporized fuel. The droplet points are contained in a rolling window, where the particles are initialized (up to 0.25 cm) ahead of the shock front as it moves ahead. In this way, the total number of Lagrangian points is kept to a minimum.

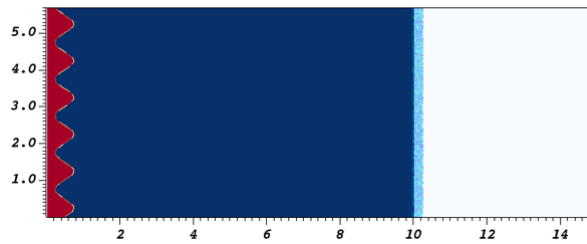


Figure 3: Simulations initial conditions. The fuel vapor phase density is plotted (red and blue) with the droplet sizes (light blue points).

Random uniform particle locations are generated with a log-normal droplet size distribution to reproduce D10 and D32 of $8.2 \mu\text{m}$ and $13.5 \mu\text{m}$ respectively. Largest size of the droplet is capped at $50 \mu\text{m}$ and a parcel size of 50 is used to generate more than six million (6,923,514) particle points, which give a global equivalence ratio (ϕ) of 0.3. Note this equivalence ratio is approximately the upper limit of that measured in the experiments.

Since the detonation is initiated with high temperature and pressure region it is initially over-driven and as it enters the multiphase region, the velocity of the detonation wave drops before it rises again as fuel droplets evaporate and fuel vapor becomes available for reaction. As the detonation wave travels through the liquid fuel region, the wave speed is not constant but it eventually settles to a quasi-steady value lower than the gaseous CJ speed. Table 2 gives the approximate average detonation wave speed obtained, which is $\sim 1.3\%$ lower than the experimental speed recorded for the same droplet size distribution. Approximate droplet evaporation distance (distance between the wave front to the point of complete evaporation of the droplets) in simulation is found to be $2 - 2.5 \text{ mm}$, which is shorter than the survival time seen in the experiments. Some droplets are found to persist for greater distances, especially near the triple points.

Table 2: Detonation Properties from Simulations and Experiments

	Wave speed (m/s)	Breakup and evaporation distance (mm)
Experiment	1794	3.55
Simulation	1770	2.0

Figure 4 shows the pressure profile and cellular structure (numerical soot foil). The cell size is predicted to be $\sim 6.7mm$ with a slightly irregular structure. This is indicative of the rapid breakup model as previous results [1] have shown much larger cell sizes with slower breakup models and similar droplet sizes. The cell size is also smaller than reported in previous experimental works, [14]. The droplet breakup region can also be observed at the right, and is seen to occur over a short distance with a few outliers falling further behind.

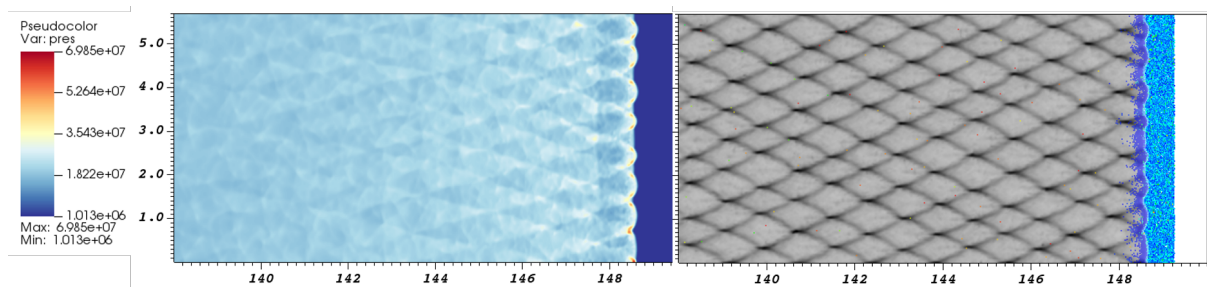


Figure 4: Simulations results at $t = 840\mu s$. Left: Pseudocolor of pressure showing the leading shock wave morphology. Right: Peak pressure history (Grey) and droplet sizes (colored points).

4 Conclusions

Experiments and simulations were performed to measure and model the droplet breakup distance in a liquid-fueled detonation. Experiments showed a rapid breakup event which occurred after an initial delay time. This behavior could be explained by an initial Kelvin-Helmholtz breakup period, which generates droplets that are too small to be observed in Mie-Scattering measurements, followed by a Rayleigh-Taylor breakup event which rapidly increases the droplet surface area (due to breakup) and allows the droplet to rapidly equilibrate with the gas flow. Simulations used a newly modified KHRT model to predict droplet survival distances at the experimental conditions. These simulation found that the droplet survival distances were smaller ($\sim 2mm$) than observed in the experiment (3.8). Further work is required to improve the KHRT model predictions. Additional experimental data could allow the KHRT model to be calibrated for detonation conditions, or improved theory could allow the model to be more accurately predicted over a wide range of conditions.

5 Acknowledgments

The authors would like to thank the Office of Naval research, award number 00014-24-1-2370, and the National Science Foundation, award number 2053154, for their support of this work.

References

- [1] Benjamin J Musick, Manoj Paudel, Praveen K Ramaprabhu, and Jacob A McFarland. Numerical simulations of droplet evaporation and breakup effects on heterogeneous detonations. *Combustion and Flame*, 257:113035, 2023.
- [2] M Pilch and CA Erdman. Use of breakup time data and velocity history data to predict the maximum size of stable fragments for acceleration-induced breakup of a liquid drop. *International journal of multiphase flow*, 13(6):741–757, 1987.
- [3] Jennifer C. Beale and Rolf D. Reitz. Modeling spray atomization with the kelvin-helmholtz/rayleigh-taylor hybrid model. *Atomization Spray*, 9(6):623–650, 1999.
- [4] Manoj Paudel and Jacob A McFarland. Equivalence ratio inhomogeneity and mixing in liquid-fueled detonations. *Fuel*, 381:133587, 2025.
- [5] Calvin J Young, Vasco O Duke-Walker, and Jacob A McFarland. Droplet breakup and evaporation in liquid-fueled detonations. *Experimental Thermal and Fluid Science*, 160:111324, 2025.
- [6] B. Fryxell, K. Olson, P. Ricker, F. X. Timmes, M. Zingale, D. Q. Lamb, P. MacNeice, R. Rosner, J. W. Truran, and H. Tufo. FLASH: An adaptive mesh hydrodynamics code for modeling astrophysical thermonuclear flashes. *The Astrophysical Journal Supplement Series*, 131(1):273–334, nov 2000.
- [7] Phillip Colella and Paul R Woodward. The piecewise parabolic method (ppm) for gas-dynamical simulations. *J. Comput. Phys.*, 54(1):174–201, 1984.
- [8] H. Wang, E. Dames, B. Sirjean, D. A. Sheen, R. Tango, A. Violi, J. Y. W. Lai, F. N. Egolfopoulos, D. F. Davidson, R. K. Hanson, C. T. Bowman, C. K. Law, W. Tsang, N. P. Cernansky, D. L. Miller, and R. P. Lindstedt. A high-temperature chemical kinetic model of n-alkane (up to n-dodecane), cyclohexane, and methyl-, ethyl-, n-propyl and n-butyl-cyclohexane oxidation at high temp+s, jetsurf version 2.0. <http://web.stanford.edu/group/haiwanglab/JetSurf/JetSurF2.0/index.html>, 2010.
- [9] David G. Goodwin, Harry K. Moffat, and Raymond L. Speth. Cantera: An object-oriented software toolkit for chemical kinetics, thermodynamics, and transport processes. <http://www.cantera.org>, 2017. Version 2.3.0.
- [10] Peter J O’Rourke and Anthony A Amsden. The tab method for numerical calculation of spray droplet breakup. Technical report, SAE technical paper, 1987.
- [11] Dionisis Stefanitsis, George Strotos, Nikolaos Nikolopoulos, Emmanouil Kakaras, and Manolis Gavaises. Improved droplet breakup models for spray applications. *International Journal of Heat and Fluid Flow*, 76:274–286, 2019.
- [12] B. Abramzon and W.A. Sirignano. Droplet vaporization model for spray combustion calculations. *Int. J. Heat Mass Tran.*, 32:1605–1618, 1989.
- [13] Rolf D. Reitz. Modeling atomization processes in high-pressure vaporizing sprays. *Atomization Spray Technol.*, 3(4):309–337, 1987.
- [14] J Papavassiliou, A Makris, R Knystautas, JHS Lee, CK Westbrook, and WJ Pitz. Measurements of cellular structure in spray detonation. *Progress in astronautics and aeronautics*, 154:148–148, 1993.